RECENT MODELLING ADVANCES FOR ULTRASONIC TOFD INSPECTIONS

Michel Darmon[a], Adrien Ferrand[a], Vincent Dorval[a], Sylvain Chatillon[a] and Sébastien Lonné[b]

[a]*CEA, LIST, DISC, F-91191 Gif-sur-Yvette cedex, France*
[b]*EXTENDE, Le Bergson, 15 Avenue Emile Baudot, F-91300 MASSY, France*

Abstract. The ultrasonic TOFD (Time of Flight Diffraction) Technique is commonly used to detect and characterize disoriented cracks using their edge diffraction echoes. An overview of the models integrated in the CIVA software platform and devoted to TOFD simulation is presented. CIVA allows to predict diffraction echoes from complex 3D flaws using a PTD (Physical Theory of Diffraction) based model. Other dedicated developments have been added to simulate lateral waves in 3D on planar entry surfaces and in 2D on irregular surfaces by a ray approach. Calibration echoes from Side Drilled Holes (SDHs), specimen echoes and shadowing effects from flaws can also been modelled. Some examples of theoretical validation of the models are presented. In addition, experimental validations have been performed both on planar blocks containing calibration holes and various notches and also on a specimen with an irregular entry surface and allow to draw conclusions on the validity of all the developed models.

Keywords: TOFD simulation, edge diffraction, lateral wave, SDH.
PACS: 43.20.Gp – 43.35.Yb – 43.35.Cg – 43.35.Pt – 43.35.Zc

INTRODUCTION

TOFD (Time Of Flight Diffraction) is a widespread NDT ultrasonic technique used for locating and sizing cracks by their diffraction echoes.
This technique relies on an arrangement of two probes of opposite beam directions. Figure 1 shows some typical phenomena arising for such an arrangement over a planar specimen containing an embedded crack-like flaw:

- Diffraction echoes (2-2') are scattered by the edges of the flaw, and caught by the receiving probe
- A lateral wave (1) is transmitted, which follows the specimen profile
- A backwall echo (3) is observed, which corresponds to the specular reflection of the beam over the outer wall of the component.

From the B-Scan image of Figure 1 one clearly distinguishes the top and bottom diffraction echoes of parabolic shapes, as well as the lateral and backwall echoes. Those echoes are conventionally used to size the defect: from the knowledge of backwall and lateral waves, beam propagation and wave speed in the material, one may straightforward estimate the locations of the edges of the flaw.

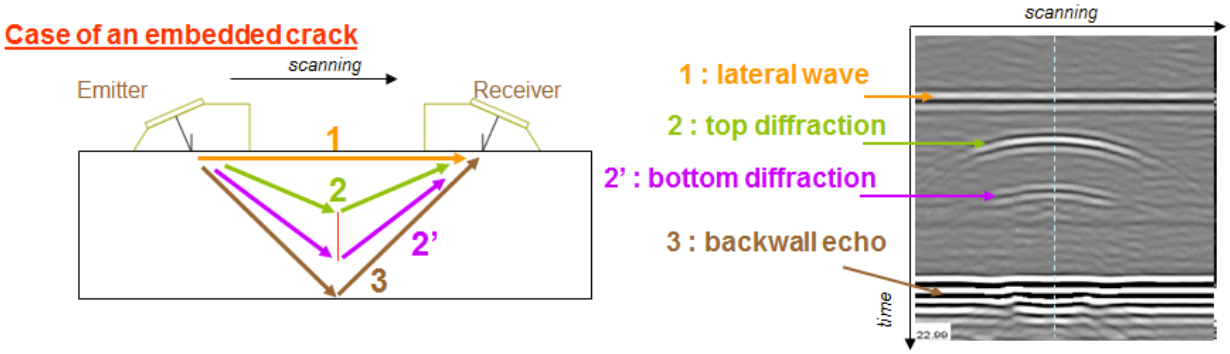

FIGURE 1. Illustration of TOFD inspection technique over a planar specimen and related echoes for an embedded crack

Depending on the size of the flaw and its position, shadowing effects over the backwall echo may arise, as the beam will be partly reflected by the flaw and lead to a lower backwall echo. This is notably the case for the configuration of a backwall breaking flaw depicted in Figure 2.

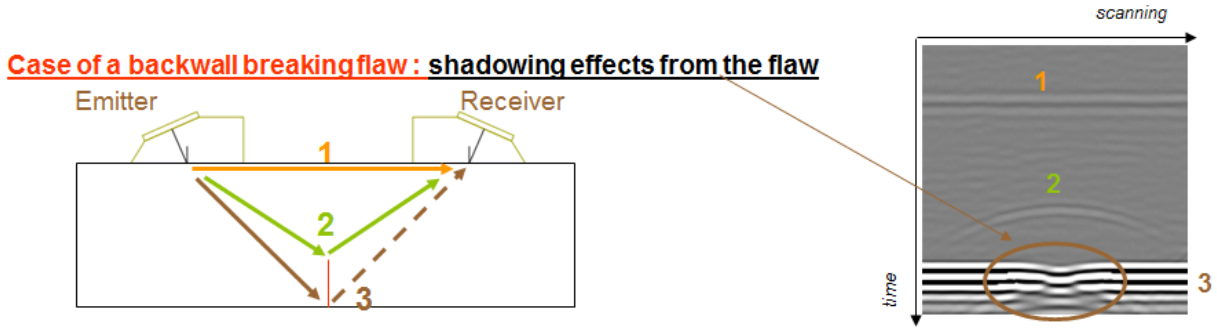

FIGURE 2. Illustration of TOFD inspection technique over a planar specimen and related echoes for a backwall breaking crack

Simulation is helpful for evaluating the performances of inspection techniques [1]. Several developments have been carried out in the past to provide, TOFD modelling in the CIVA software. Simulation of TOFD inspection henceforth involves the necessary simulation of complex phenomena due to the 3D geometries of flaws and structures. Consequently several improvements have been newly integrated in the TOFD simulation tools.

LATERAL WAVES

So as to simulate lateral waves, two different developments have been devised. The first one is devoted to planar components: it was previously added to CIVA and recently improved. The second one is newly developed and dedicated to lateral waves on irregular surfaces; the validation of its complete process has to be successfully finished.

Lateral Waves on Planar Components

Concerning the simulation of lateral waves on planar components, the main recent improvement has consisted in the replacement of the previous 2D model [2] by a 3D one. Such a simulation tool follows a procedure depicted in Figure 3:

1) Discretization of transmitting and receiving surfaces into elementary surfaces surrounding mesh points P_i and P_j

2) Between two points P_i and P_j, respectively located on the emitting and receiving surfaces:

Calculating the 3D path of the lateral head wave (HW).

Application of asymptotic ray theory (Cerveny's model [2]) for calculating each ray amplitude.

3) Frequency loop and summation over the transmitter and receiver surfaces.

The lateral wave is also called head wave since it is the first arrival wave received during a TOFD (Time Of Flight Diffraction) inspection. For a planar surface, a head wave is generated at critical incidence at the interface between the material and the emitter, propagates in the material along the surface, and is radiated at critical angle as a bulk wave in the wedge, reaching the receiver. For planar surfaces, the head wave is seen as the result of a critical refraction phenomenon of the incident wave on the interface between the two media.

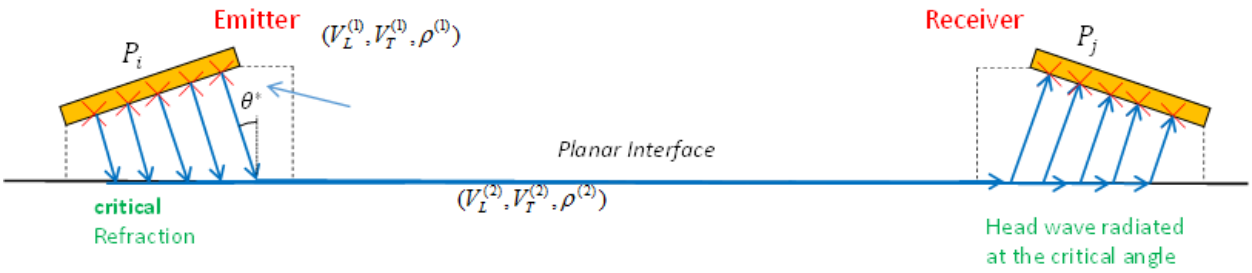

FIGURE 3. Procedure for simulating lateral waves on planar components using contact probes.

Previously the head wave amplitude was computed by summing contributions from only 2D paths aligned along the axis connecting the two probes centers [2]. In the framework of the 3D new model for lateral waves on planar components, the paths of the lateral wave are calculated in 3D; consequently the contribution of some new rays skewed with respect the probe centers axis is truly taken into account. Numerical and experimental validations are in progress.

Shadowing by a near surface crack

In TOFD inspections, a surface breaking flaw prevents the lateral wave to be transmitted from one probe to the other (Figure 4 left). That's why head waves can sometimes be used for surface breaking cracks detection.

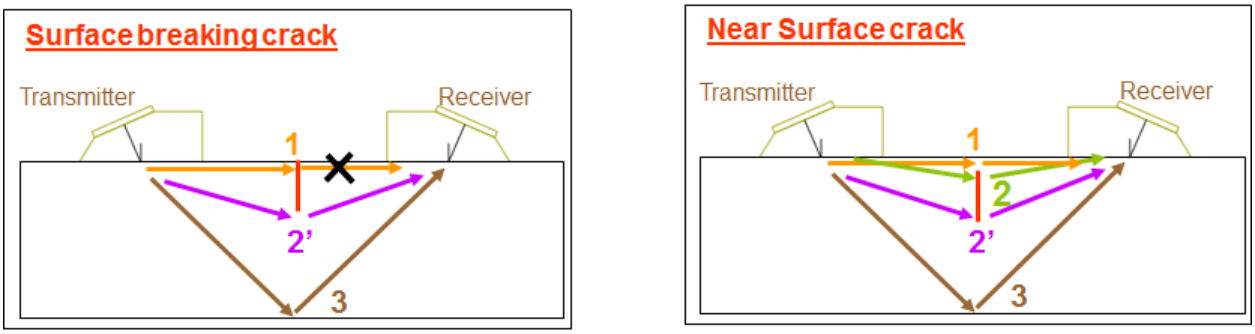

FIGURE 4. TOFD inspections on a planar component: at left, case of a surface breaking crack; at right, case of a near surface crack.

On the other hand, when the crack is located near the surface and separated from it by a distance called ligament, complex interferences between the head wave and the top edge diffracted wave occur. There is not anymore interruption of the lateral wave but there is still an effect of the ligament on the lateral wave amplitude.

To model this ligament effect, an empirical model which has been integrated in CIVA11 release has been developed to simulate, in a simplified manner, the interferences between the head wave and the top edge diffraction. An amplitude law for the head wave amplitude has been adjusted using CIVA/ATHENA [4] finite elements calculations as reference:

$A_{HW} = A_{HW0}\left(\frac{l_{ligament}}{l_c}\right)^2$ where A_{HW0} is the simulated lateral head wave without flaw, $l_{ligament}$ is the ligament and $l_c = 3\sqrt{\lambda}$ where λ is the wavelength.

Thanks to this empirical adjustment of the amplitude law, this simplified model leads for several metallic materials to results similar to finite elements ones except for ligaments close to the critical ligament l_c.

Examples of simulations of the lateral wave using this empirical model are given hereafter. Analytical Civa simulations have been performed for TOFD inspections on a plane specimen using two identical probes with a 70mm Probe Center Space (PCS) emitting P60° waves at 2MHz. The specimen contains a flaw of fixed bottom edge location but varying ligament.

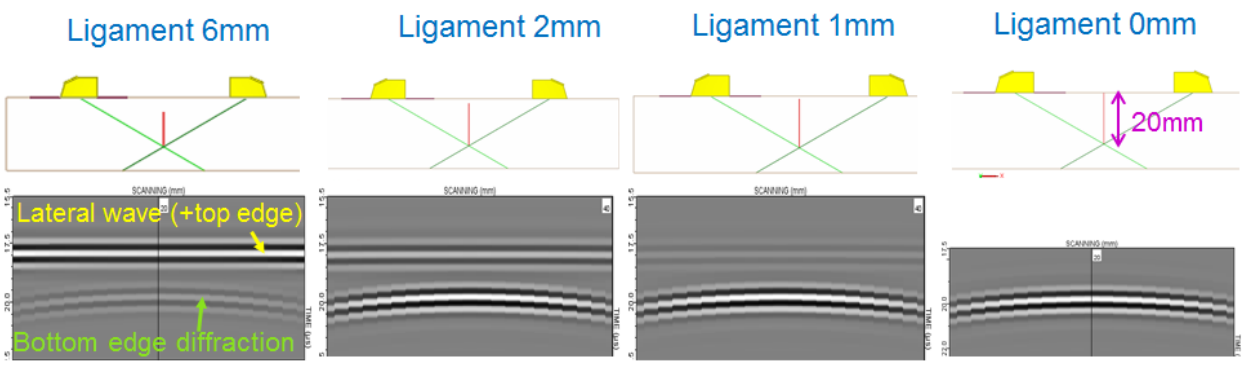

FIGURE 5. CIVA Simulations of TOFD inspections on a planar component containing a flaw of fixed bottom edge location but varying ligament (from 6 to 0 mm).

For 6 mm ligament, a total transmission of the lateral wave is observed and there is no flaw influence on the head wave. When decreasing the ligament, a decrease of the HW amplitude is predicted, the HW becoming less predominant than the bottom edge diffraction echo. When the flaw is a surface breaking one, a total interruption of the lateral wave is modelled and the bottom edge diffraction echo is the only observed one.

The simulation provides thus a progressive extinction of the lateral wave with a decreasing ligament.

Lateral Waves on Irregular Surfaces

TOFD and other pitch-catch configurations are also classically used on non-planar interfaces in NDE (inspections of cylinders, nozzles [3]…).

The previously developed model for head waves simulation is based on the asymptotic ray theory [2] which has also been used to improve the modeling of flaw corner echoes [4]. Nevertheless, this existing head wave simulation can only be applied for a planar specimen composed of an isotropic medium.

In [5], complete interpretation and simulation of the head wave propagation mechanisms for irregular surfaces are proposed. This approach leads to the development of a generic algorithm of ray tracing between interface points (called Generic Interface Ray Tracing/GIRT) which is able to compute the travel path of head waves in specimens inspected by TOFD technique. Based on an adaptation to the NDE domain of seismic ray tracing algorithms, GIRT is a new method for solving the two-points ray tracing problem, which is the calculation of the true ray between two defined points: the source and observation ones.

The GIRT algorithm is adapted to find not only the head wave ray path (first arrival) but also all complex later arrival waves including mode or nature conversion by adding constraints on the searched ray path. Secondly, GIRT can take into account all types and natures of waves propagation occurring in NDE. Indeed the propagation simulation is available for both P and SV waves and accounts for modes conversions. Surface waves as Rayleigh waves and head waves are taken into account as well as diffractions from surfaces in any kind of waves. Finally, GIRT approach is extended to flaw scattering modeling since the flaws contained in the specimen are also meshed by the GIRT algorithm in order to model rays diffracted from flaws. Consequently the GIRT algorithm is generic for application to NDE as it can deal with any ultrasonic wave propagating near irregular surfaces or flaws of any geometry (CAD defined).

By modeling the complex wave interactions with the surfaces thanks to this ray approach, GIRT is thus able to correctly predict the head wave time of flight and to interpret the complex waves propagation at the vicinity of an irregular interface. Indeed, comparisons between GIRT and FEM simulations of the head wave fronts near the receiver surface have been previously presented in [5]. A good agreement is obtained between GIRT and FEM results, which validates the GIRT algorithm. For very corrugated surfaces, a bulk propagation mechanism has to be taken into account for the head wave modeling. GIRT has been integrated in CIVA11 release to predict the valid time of flight for lateral waves on irregular surfaces.

A 2D model for simulating precisely the lateral waves amplitude on irregular surfaces has then been devised; it has not been yet integrated in CIVA, its validation being in progress. For the moment, this model can deal with cylindrical (Figure 6) or scouring irregularities (Figure 7). The computation of head wave amplitude is derived from ray-based models.

The head wave ray path is determined by GIRT between source and observation points located over the probes surfaces. The ray path is divided into elementary paths and the application of an amplitude ray model for each interaction corresponding to each elementary path is carried out. Two specific new ray models have been developed: one to simulate the creeping ray along a cylindrical part and one to model a grazing ray along a planar part (Figure 7). Indeed, these two elementary paths are involved in the head wave path on scoured surfaces.

The developed models and their validations will be described in a future publication. Encouraging results have been obtained for simulating 2D lateral waves on cylindrical or scoured surfaces.

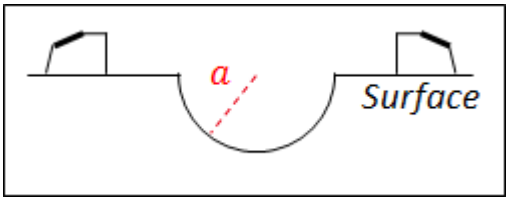

FIGURE 6. Cylindrical irregularity of radius a.

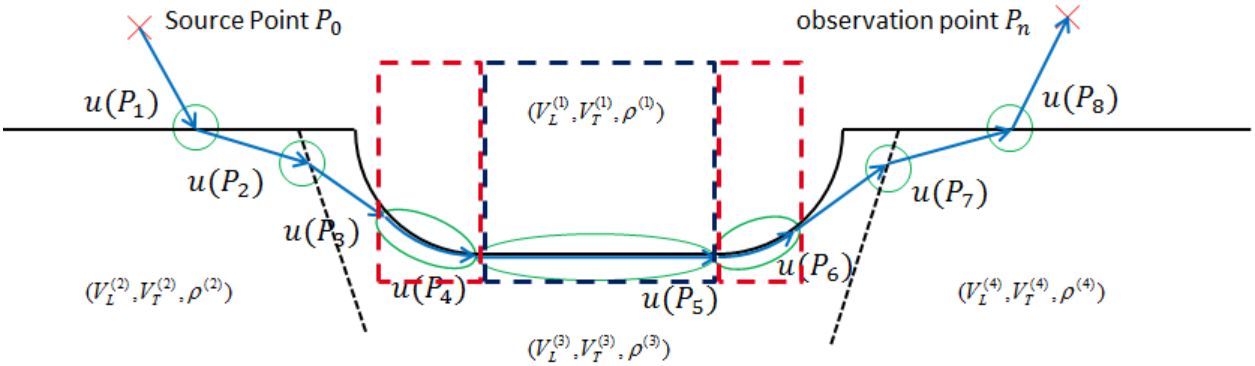

FIGURE 7 Amplitude calculation along a ray path calculated by GIRT over a scoured irregularity. Red dashed blocks: creeping ray along cylindrical parts. Blue dashed block: grazing ray along the planar part.

CRACK DIFFRACTION

In order to predict TOFD inspection performance in realistic configurations, the simulation needs to account for arbitrarily oriented flaws with respect to the probes orientation. In addition to tilt angle (flaws not necessarily perpendicular to a planar backwall), skew or vertical disorientation angles may apply, for instance using inspection over pipes or nozzles. Moreover, realistic flaws, may have a complex contour shape (not necessarily rectangular aperture), so developments were also carried out to account for CAD contour planar flaws and in addition branched or multifaceted flaws. Edge diffraction echoes can be modelled identically by GTD or new PTD [6] [7] models. Two different strategies have been investigated concerning the calculation of the GTD coefficients. A so-called "projected 2D" option, which is based onto the projection of the incoming and scattered wave vectors over the plane which contains the normal of the flaw edge, was previously available. It has been removed and replaced in CIVA11 release by a "pure" 3D GTD code, (metre une reference). The advantages of the 3D codes are a better prediction for strong 3D crack misorientation and the use of a new TV-TH decomposition: continuous limit when turning the 3D problem into 2D one.

An example of experimental validation of the GTD model implemented in CIVA is performed hereafter. The reference block, of 30mm thickness, is composed of steel and incorporates 11 artificial notches of extension 15mm and heights varying from 0.5mm to 15mm (Figure 8).

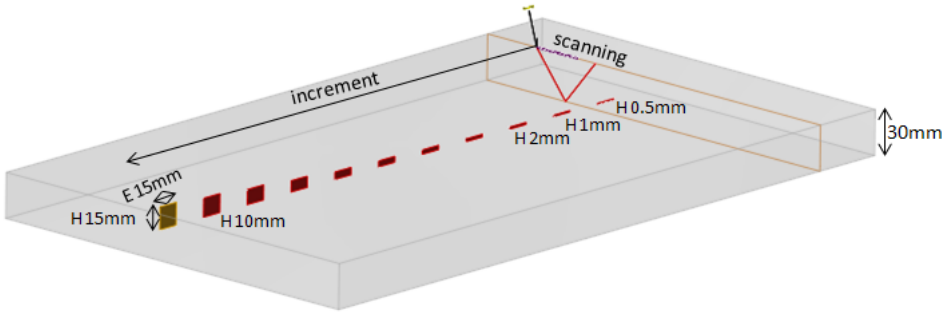

FIGURE 8*:* Steel specimen, 30 mm thickness, with back-wall breaking artificial notches of height 0.5mm, 1mm, 1.5mm, 2mm, 3mm, 4mm, 5mm, 7.5mm, 10mm, 12.5mm and 15mm (15 mm extension).

The material homogeneity was experimentally checked and the specimen material (steel) was modelled as isotropic, homogeneous and the attenuation was ignored. The longitudinal (L) and transversal (T) velocities were estimated using successive backwall echoes (V_L = 5900m.s^{-1} and V_T = 3230m.s^{-1}), the density was 7.8g.cm^{-3}.

The two probes arranged in TOFD mode were moved in two directions over the notches with a scanning step of 0.2 mm and an increment step of 1mm. The probes used were single element conventional round probes with a centre frequency of 5MHz and a diameter of 6.35mm. Concerning the material properties of the wedges, the longitudinal and transversal velocities are respectively V_L = 2730m.s^{-1} and V_T = 1340m.s^{-1} and the density is 1.18g.cm^{-3}.

TOFD inspection of the back-wall breaking notches was performed for probe centre space "PCS" (Figure 9) varying from 35mm to 100mm, allowing various incidence angles of the L waves on the top edge and various positions of the "L axis crossing point" (point where the L axis of the transmitter and receiver intersect) relative to that of the top edge (Figure 9).

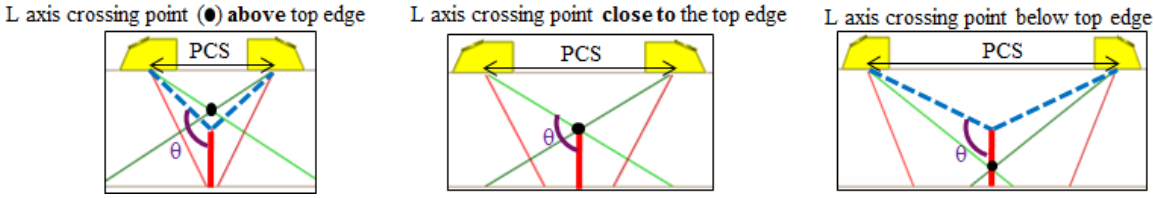

FIGURE 9*:* CIVA schematics of TOFD configurations with different PCSs, showing the variation of the L waves incident angle on the top edge of the notch (θ) and of the L axis crossing point position relative to that of the top edge with the PCS.

Figure 10 shows the experimental and simulated amplitudes of the top edge echo obtained for the TOFD inspection of the 15mm height notch performed with the probes generating longitudinal waves at 60° in the specimen and for various PCS. Three different simulations are shown: one using GTD model and two simulations using the finite elements model CIVA/ATHENA [8] both for a null or 0.2mm notch aperture. The reference for the amplitude is the L direct echo of the SDH Ø2mm at 20mm depth obtained in TOFD mode with a PCS of 70mm.

When the PCS increases, the "L axis crossing point", located above the top edge for the PCS of 35mm, moves deeper, reaches the top edge for PCS = 50 mm and then drops below it. The amplitude of the top edge echo reaches its maximum when the crossing point is close to the top edge.

We have a good agreement between experiment and GTD or CIVA-ATHENA predictions whatever the notch aperture. In this case, we observe almost no effect of the notch aperture. Indeed we can see on the right of Figure 10 that, whatever the PCS, the incident angle θ is less than 130°, and influence of the notch aperture on the top edge echo amplitude occurs only for θ angles greater than 130°. Differences between GTD and CIVA-ATHENA appear for such angles owing to an additional specular echo coming from the horizontal part of the notch top. Contrary to CIVA-ATHENA, the GTD model does not compute this specular echo.

The same good agreement between experiments and the three simulations (with GTD and CIVA-ATHENA with quasi null or 0.2mm aperture) was obtained for the notches of 10mm and 5mm.

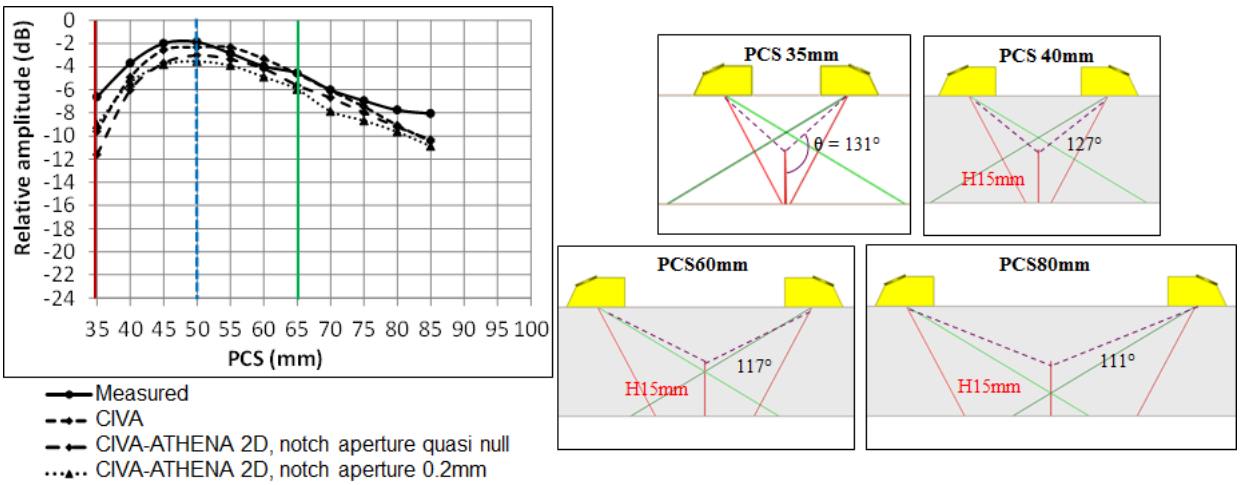

FIGURE 10*:* L60° TOFD inspection, notch of 15mm height. Left) Compared experimental and simulated amplitudes of the L top edge echo versus the PCS. Three different simulations shown: one using CIVA GTD model and two simulations using the finite elements model CIVA/ATHENA both for a null or 0.2mm notch aperture. Right) Inspection configurations for different PCS showing the relative positions of the notch and the probes.

CALIBRATION DEFECTS

Until CIVA10 release, the response of a side drilled hole (SDH) which is a classical calibration flaw was only modelled using the Kirchhoff approximation: it takes into account specular reflection on a cavity but not the creeping waves which propagate around the cavity circumference (Figure 13). Therefore, an exact analytical solution for the scattering from a cylindrical cavity, based on the Separation Of Variables (SOV) method [8], has been implemented in CIVA 10 to improve simulation of the SDH response [9].

For validation purposes, TOFD inspections of a planar block containing SDHs were performed by varying the PCS of 50mm to 80mm. When the PCS increases, L theoretical axes of the two sensors intersect above and below the TG of different diameters located at 20mm deep. The crossing point is at the SDH depth when the PCS is about 70mm. These axes and the angles of incidence on the TG are shown in Figure 11.

FIGURE 11*:* SDH at 20mm depth, ray path display and value of the direct ray incidence angle on the SDH. TOFD inspection, contact probe Ø6.35mm, 5MHz, P60°, various PCS.

Experimental Ascans, measured on a Ø2mm SDH located at 20mm depth are compared to simulated ones, using SOV model, for different PCS.

The SOV model predicts the existence of the two SDH echoes (specular reflection and creeping wave) but their relative amplitudes are not always perfectly correct: in the case of small PCS, 50mm or 60mm) for which the intersection point of axes is above the SDH, the second echo is overestimated by CIVA. When the depth of the intersection point is on the SDH the amplitudes of two echoes (which are similar) are very well predicted. Nevertheless, the maximal amplitudes obtained with CIVA10 for this Ø2mm SDH versus the PCS are always in good agreement with those measured even for PCS 50mm or 60mm when the amplitude of the second echo is not correct (Figure 12) because its amplitude, smaller than the first echo, does not really affect the measurement of the maximum amplitude of the SDH echo. For more important PCS, there is more field amplitude on the SDH bottom; moreover, when increasing the PCS as shown in Figure 13, the path for creeping waves is shorter and their attenuation is smaller. Consequently the creeping waves amplitude increases with the PCS.

Improvement due to creeping waves modelling (not accounted in Kirchhoff model) is henceforth obtained using the CIVA SOV model.

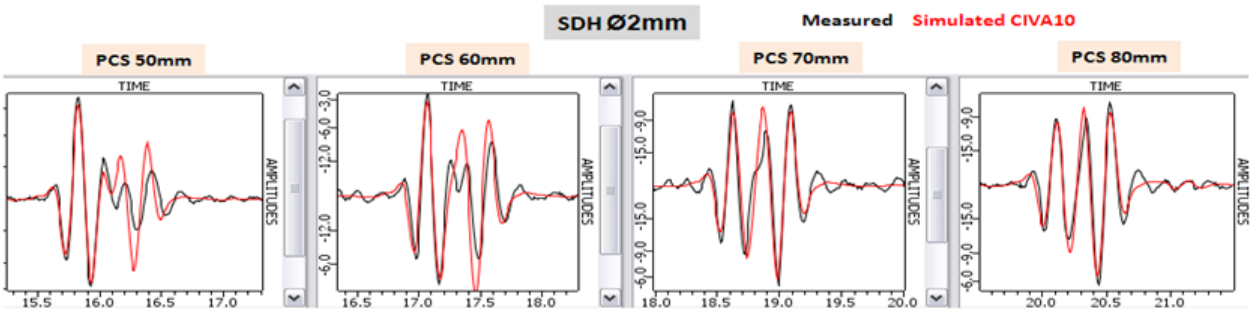

FIGURE 12: Comparison of measured (black) and simulated with CIVA Ascans from a 2mm diameter SDH for different diameters PCS. TOFD inspection with Ø6.35mm probe, 5MHz, P60°.

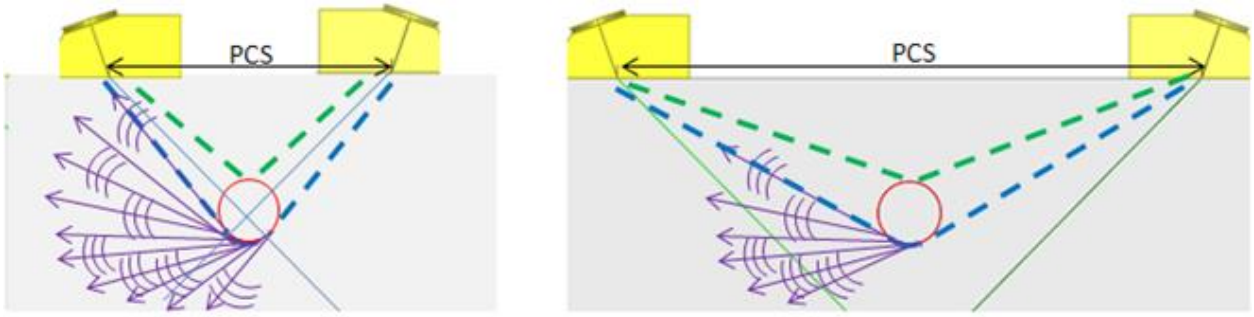

FIGURE 13: Specular path (in green) and creeping wave path (in blue) around the side drilled hole which is shorter for great PCS than for the little corresponding to a weaker energy loss by irradiation along this path.

CONCLUSION

Recent developments have been carried out to enhance the abilities of ultrasonic TOFD inspection simulation. New SOV exact analytical model enables to improve simulation of a typical calibration flaw, a SDH, by accounting for creeping waves. Lateral waves on planar components are henceforth simulated using a 3D model and accounting their shadowing by a near surface crack. A 2D model of lateral waves on irregular surfaces has also been devised for cylindrical or scoured irregularities. Intensive experimental validations of all these improvements are in progress. Simulation of lateral waves on irregular surfaces could be further improved to deal with 3D configurations, wedge-like irregularities, impedance interfaces and anisotropic media. So as to simulate edge diffraction, integration of 3D GTD model and of the generic PTD has been performed leading to successful validations. Works are in progress to improve edge diffraction simulation near critical angles.

REFERENCES

1. M. Darmon et S. Chatillon, *Open Journal of Acoustics*, **3A**, 2013.
2. V. Cerveny et R. Ravindra, *Theory of seismic head waves*, University of Toronto Press (Toronto), 1971.
3. S. Chaffai, M. Darmon, S. Mahaut et R. Menand, «Simulations tools for TOFD inspection in Civa software,» ICNDE 2007, 2007.
4. S. Mahaut, G. Huet et M. Darmon, « Modeling of Corner Echo in UT Inspection Combining Bulk and Head Waves Effect,» 35th Annual Review of Progress in Quantitative Nondestructive Evaluation , 2009.
5. A. Ferrand, M. Darmon, S. Chatillon et M. Deschamps, *Ultrasonics*, **54**, 7, pp 1851–1860, 2014
6. V. Zernov, L. Fradkin et M. Darmon, *Ultrasonics*, **52**, 17, pp. 830-835, 2012.
7. V. Dorval, M. Darmon, S. Chatillon et L. Fradkin, «Simulation of the UT inspection of planar defects using a generic GTD-Kirchhoff approach,» in Review of Progress in Quantitative Nondestructive Evaluation, Boise, 2014.
8. M. Darmon, N. Leymarie, S. Chatillon et S. Mahaut, «Modelling of scattering of ultrasounds by flaws for NDT,» in *Ultrasonic wave propagation in non homogeneous media*, vol. 128, Springer Berlin, 2009, pp. 61-71.
9. M. Darmon, S. Chatillon, S. Mahaut, P. Calmon, L. Fradkin et V. Zernov, Journal of Physics: Conference Series, 269, 1, pp. 012013 (12 pp.), 2011.